1P3-4

Proceedings of Symposium on Ultrasonic Electronics, Vol. 36 (2015)
5-7 November, 2015

Study on Generation Mechanisms of Third-order Nonlinear Signals in SAW Devices on the Basis of Simulation

シミュレーションに基づく SAW デバイスの 3 次非線形信号発生メカニズムに関する研究

Ryo Nakagawa[1,2†], Takanao Suzuki[1], Hiroshi Shimizu[1], Haruki Kyoya[1], Katsuhiro Nako[1], and Ken-ya Hashimoto[2]
([1]Murata Manufacturing Co., Ltd.; [2]Grad. School of Eng., Chiba Univ.)
中川 亮 [1,2†]，鈴木 孝尚 [1]，清水 寛司 [1]，京屋 治樹 [1]，名古 克裕 [1]，橋本 研也 [2]
([1] 村田製作所, [2] 千葉大院 工)

1. Introduction

Recently, linearity improvement is one of the most important subjects in the research and development of SAW and BAW devices. In this situation, better understanding of the generation mechanisms of nonlinear signals are crucial.

In this work, we discuss the generation mechanisms of third-order nonlinearity in SAW devices. For this discussion, simulation method of nonlinear signals, in which conceivable all generation mechanisms of nonlinearity are taken into account, is proposed. As the result of comparisons of simulation results and measured data, it is shown that contributions of each mechanism to nonlinear signals change markedly with the input and output frequency conditions.

2. Simulation Method of Nonlinear Signals

First, an analysis model used in this method is shown in Fig. 1. This model has multiple excitation and receiving points to express the wave excitation and pick up by an inter-digital transducer on piezoelectric substrate.

By introducing nonlinear terms into the piezoelectric constructive equation, nonlienar stress T_{N} and nonlinear current I_{N} generated by third-order nonlinearrity at each receiving point l in the case of simultaneous two signals input are expressed as forrows[1)]:

$$
\begin{aligned}
T_{\mathrm{N}l}^{(2\omega_1 \pm \omega_2)} = j\frac{1}{\omega_1^2 \omega_2}\Big[&\mu_{\mathrm{m}}^{(03)} \hat{I}_l^{(\mathrm{A})}(\omega_1)^2 \hat{I}_l^{(\mathrm{A})}(\omega_2) \\
&+ \mu_{\mathrm{m}}^{(12)}\left\{2\hat{I}_l^{(\mathrm{A})}(\omega_1)\hat{I}_l^{(\mathrm{E})}(\omega_1)\hat{I}_l^{(\mathrm{A})}(\omega_2) + \hat{I}_l^{(\mathrm{A})}(\omega_1)^2 \hat{I}_l^{(\mathrm{E})}(\omega_2)\right\} \\
&+ \mu_{\mathrm{m}}^{(21)}\left\{2\hat{I}_l^{(\mathrm{A})}(\omega_1)\hat{I}_l^{(\mathrm{E})}(\omega_1)\hat{I}_l^{(\mathrm{E})}(\omega_2) + \hat{I}_l^{(\mathrm{E})}(\omega_1)^2 \hat{I}_l^{(\mathrm{A})}(\omega_2)\right\} \\
&+ \mu_{\mathrm{m}}^{(30)} \hat{I}_l^{(\mathrm{E})}(\omega_1)^2 \hat{I}_l^{(\mathrm{E})}(\omega_2)\Big],
\end{aligned}
$$

$$
\begin{aligned}
I_{\mathrm{N}l}^{(2\omega_1 \pm \omega_2)} = -\frac{2\omega_1 \pm \omega_2}{\omega_1^2 \omega_2}\Big[&\mu_{\mathrm{e}}^{(03)} \hat{I}_l^{(\mathrm{A})}(\omega_1)^2 \hat{I}_l^{(\mathrm{A})}(\omega_2) \\
&+ \mu_{\mathrm{e}}^{(12)}\left\{2\hat{I}_l^{(\mathrm{A})}(\omega_1)\hat{I}_l^{(\mathrm{E})}(\omega_1)\hat{I}_l^{(\mathrm{A})}(\omega_2) + \hat{I}_l^{(\mathrm{A})}(\omega_1)^2 \hat{I}_l^{(\mathrm{E})}(\omega_2)\right\} \\
&+ \mu_{\mathrm{e}}^{(21)}\left\{2\hat{I}_l^{(\mathrm{A})}(\omega_1)\hat{I}_l^{(\mathrm{E})}(\omega_1)\hat{I}_l^{(\mathrm{E})}(\omega_2) + \hat{I}_l^{(\mathrm{E})}(\omega_1)^2 \hat{I}_l^{(\mathrm{A})}(\omega_2)\right\} \\
&+ \mu_{\mathrm{e}}^{(30)} \hat{I}_l^{(\mathrm{E})}(\omega_1)^2 \hat{I}_l^{(\mathrm{E})}(\omega_2)\Big],
\end{aligned}
$$

----
r_nakagawa@murata.com

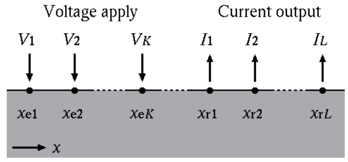

Fig. 1 Analysis Model.

where, ω_1 and ω_2 are angular frequencies of input singnals, and $\mu_{\mathrm{m}}^{(ij)}$ and $\mu_{\mathrm{e}}^{(ij)}$ are nonlinear coefficients. In particular, $\mu_{\mathrm{m}}^{(03)}$ and $\mu_{\mathrm{e}}^{(30)}$ represent the nonlinear elasticity and dielectrics, respectively, while the others represent the nonlinearity of electromechanical coupling. In addition, $\hat{I}_l^{(\mathrm{A})}$ and $\hat{I}_l^{(\mathrm{E})}$ are linear currents at acoustic pass and electric pass, respectively, and they can be derived from linear case analysis such as coupling of modes theory[2)]. Therefore, provided that the nonlinear coefficients $\mu_{\mathrm{m}}^{(ij)}$ and $\mu_{\mathrm{e}}^{(ij)}$ are determined *a priori*, the nonlinear stress and the nonlinear current can be calculated by using only the results of a conventional linear analysis.

Nonlinear signal levels at external terminals of a terget device are estimated by giving obtained nonlinear stresses and nonlinear currents into an equivalent circuit of it as the voltage and current sources as shown in Fig. 2.

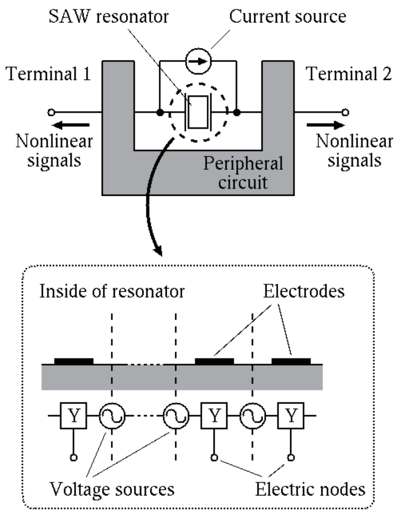

Fig. 2 Estimation of Nonlinear Signal Level.

3. Simulation and discussion

Fig. 3 shows experimental and fitted simulation data of third-order harmonics (H3) and intermodulation distortion (IMD3) $2f_1$-f_2 of a one-port SAW resonator. Resonance frequency f_r and anti-resonance frequency f_a of the fabricated resonator are 835 and 863 MHz, respectively. In the measurement of H3, input frequency was swept from 800 to 900 MHz, and output signal appeared at 2.4 to 2.7 GHz was detected. On the other hand, in the measurement of IMD3, two input signals with frequencies f_1 and f_2 were applied simultaneously. Frequency f_1 was swept from 824 to 849 MHz, while f_2 was swept to be f_1-45 MHz. Then, output signal $2f_1$-f_2 appeared at 869 to 894 MHz was detected. In these measurements, powers of input signals at the input terminal were set at 15 dBm. In Fig. 3, simulated data agree well with measured data. For all calculations, identical nonlinear coefficients were used. This indicates validity of the proposed model.

Fig. 4 shows the contributions of each nonlinear term to the simulation results given in Fig. 3. For the case of H3 in Fig. 4(a), effects of $\mu_e^{(03)}$, $\mu_e^{(21)}$, and $\mu_e^{(30)}$ are dominant. In this case, since input signal f_1 is close to f_r, the effect of the coefficient $\mu_e^{(03)}$ representing acoustic nonlinearity is significant. On the other hand, in the case of IMD3 in Fig. 4(b), the characteristics is mostly governed by the effect of $\mu_m^{(03)}$. This is because all of two input signals and output signals are close to f_r and thus acoustic waves are excited and detected efficiently for both the linear and nonlinear signals.

As shown in Fig. 4, significances of each nonlinear term to the nonlinear responses are change markedly depending on the driving conditions. In this case, it was shown that influences of I_N is dominant for the out-band nonlinear signal output while T_N is significant when a nonlinear signal is generated close to f_r.

4. Conclusion

In this work, generation mechanisms of third-order nonlinearity are discussed by using the simulation method proposed for this discussion. The simulation results showed very good agreement with measured data when the nonlinear coefficients were properly determined. In addition, it was shown that the significances of each nonlinear coefficient are change markedly depending on the driving condition.

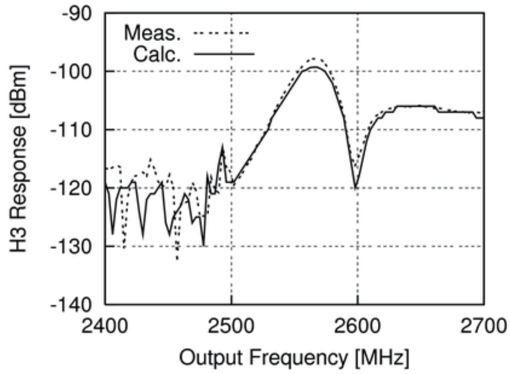

(a) H3

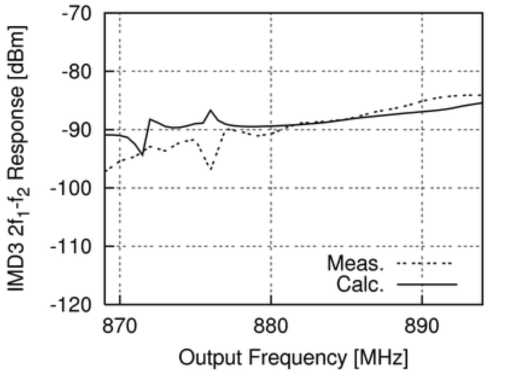

(b) IMD3 $2f_1$-f_2

Fig. 3 Measured and Simulated Results of H3 and IMD3.

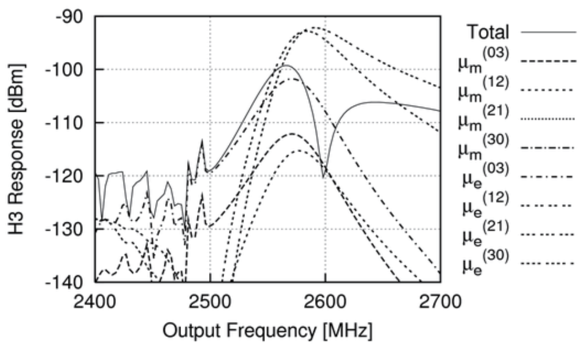

(a) H3

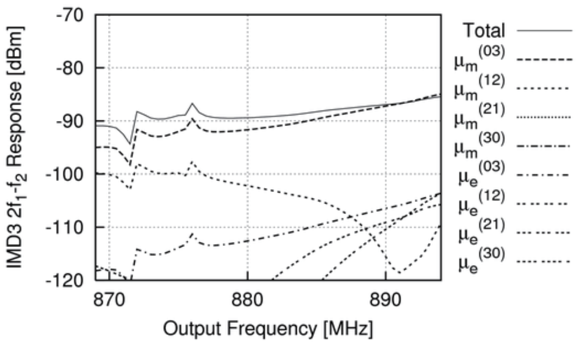

(b) IMD3 $2f_1$-f_2

Fig. 4 Influence of Each Nonlinear Coefficient to Nonlinear Signals.

References

1. R. Nakagawa, T. Suzuki, H. Shimizu, H. Kyoya, and K. Nako: EuMiC, pp. 292-295, Oct. 2013.
2. K. Hashimoto, *Surface Acoustic Wave Devices in Telecommunications*, Springer Verlag, 2000, p.191.